



**Small-Molecule Inhibitor of *Vibrio cholerae*
Virulence and Intestinal Colonization**

Deborah T. Hung, *et al.*
Science **310**, 670 (2005);
DOI: 10.1126/science.11116739

***The following resources related to this article are available online at
www.sciencemag.org (this information is current as of May 7, 2007):***

Updated information and services, including high-resolution figures, can be found in the online version of this article at:

<http://www.sciencemag.org/cgi/content/full/310/5748/670>

Supporting Online Material can be found at:

<http://www.sciencemag.org/cgi/content/full/1116739/DC1>

This article **cites 18 articles**, 9 of which can be accessed for free:

<http://www.sciencemag.org/cgi/content/full/310/5748/670#otherarticles>

This article has been **cited by** 17 article(s) on the ISI Web of Science.

This article has been **cited by** 11 articles hosted by HighWire Press; see:

<http://www.sciencemag.org/cgi/content/full/310/5748/670#otherarticles>

This article appears in the following **subject collections**:

Microbiology

<http://www.sciencemag.org/cgi/collection/microbio>

Information about obtaining **reprints** of this article or about obtaining **permission to reproduce this article** in whole or in part can be found at:

<http://www.sciencemag.org/about/permissions.dtl>

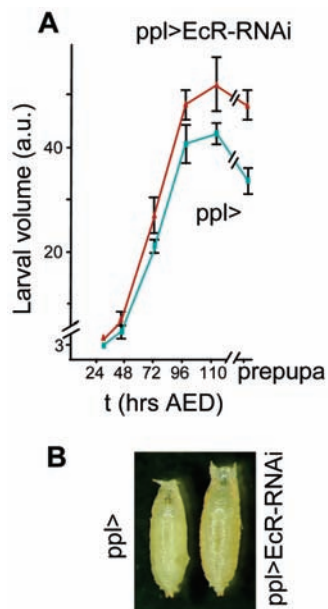


Fig. 4. The larval fat body relays the 20E-dependent growth inhibitory signal to larval tissues. The *ppl*-Gal4 driver (*ppl*>) allows specific expression of *EcR*-RNAi constructs in the larval fat body. (A) Measurement of larval volumes ($n = 10$ per time point). (B) Size difference between control and *pplGal4>EcR-RNAi* prepupae (120 hours AED).

dominant-negative form of *EcR* (*EcR^{F645A}*) (18). In these conditions, we observed a reduced accumulation of *dFOXO* in the nuclei of *EcR^{F645A}*-expressing cells (Fig. 3D). As an expected consequence, global accumulation of *4E-BP* transcripts was consistently higher in *P0206>PI3K* as well as in 20E-fed early L3 larvae relative to control animals, and was reduced upon general *EcR* silencing (*arm>EcR-RNAi*) (Fig. 2E). Together, these results indicate that ecdysone-dependent inhibition of larval growth correlates with a general alteration of insulin/IGF signaling and a relocalization of *dFOXO* into the cell nuclei. To more directly test the role of *dFOXO* in the growth-inhibitory function of ecdysone signaling, we examined the effects of increasing ecdysone levels in a *dFOXO* mutant genetic background. Although homozygous *dFOXO²¹* animals do not display a detectable growth phenotype (Fig. 2F) (16), introducing the *dFOXO²¹* mutation was sufficient to totally reverse the growth defects of *P0206>PI3K* animals, either homozygous (Fig. 2F) or heterozygous (9). These data establish that *dFOXO* is required for 20E-mediated growth inhibition.

The endocrine activities of the brain and the fat body have previously been implicated in the humoral control of larval growth (19, 20). To test for possible roles of these two organs in mediating the systemic growth effects of ecdysone, we silenced *EcR* expression specifically in the brain's insulin-producing cells (IPCs) or in the fat body. Whereas spe-

cific expression of *EcR* RNAi in the IPCs failed to reproduce the overgrowth observed in *armGal4>EcR-RNAi* animals (9), *EcR* silencing in the fat body elicited an acceleration of larval growth and a remarkable increase in pupal size (Fig. 4, A and B). Moreover, no detectable delay was observed in the larval timing of these animals (Fig. 1C). Thus, specifically reducing 20E signaling in the fat body is sufficient to recapitulate the systemic effects of global *EcR* silencing. Hence, the fat body is a major target for ecdysone, and this tissue can act to relay the 20E growth-inhibitory signal to all larval tissues.

Our results establish an additional role for 20E in modulating animal growth rates. This function is mediated by an antagonistic interaction with IIS that ultimately targets *dFOXO* function (fig. S2E). A similar antagonistic interaction between 20E and insulin signaling was recently shown to control developmentally regulated autophagy in *Drosophila* larva (21).

Although we do not rule out a direct effect of ecdysone on the cellular growth rate of all larval tissues, our experiments reveal a key role for the fat body in relaying ecdysone-dependent growth control signals. Together with previous work (3), these data suggest that various inputs such as nutrition and ecdysone converge on this important regulatory organ, which then controls the general IIS to modulate organismal growth (fig. S2E). How, then, is growth connected to developmental timing? Our finding that 20E can modulate growth rates in addition to developmental transitions places this hormone in a central position for coordinating these two key processes and controlling organismal size.

References and Notes

1. E. Hafen, *Curr. Top. Microbiol. Immunol.* **279**, 153 (2004).
2. J. S. Britton, W. K. Lockwood, L. Li, S. M. Cohen, B. A. Edgar, *Dev. Cell* **2**, 239 (2002).
3. J. Colombani et al., *Cell* **114**, 739 (2003).
4. L. M. Riddiford, *Receptor* **3**, 203 (1993).
5. H. F. Nijhout, *Dev. Biol.* **261**, 1 (2003).
6. D. Stern, *Curr. Biol.* **13**, R267 (2003).
7. G. Adam, N. Perrimon, S. Noselli, *Development* **130**, 2397 (2003).
8. W. Janning, *Semin. Cell Dev. Biol.* **8**, 469 (1997).
9. J. Colombani et al., data not shown.
10. J. P. Parvy et al., *Dev. Biol.* **282**, 84 (2005).
11. F. D. Karim, C. S. Thummel, *Genes Dev.* **5**, 1067 (1991).
12. V. M. Chavez et al., *Development* **127**, 4115 (2000).
13. J. T. Warren et al., *Insect Biochem. Mol. Biol.* **34**, 991 (2004).
14. L. A. Johnston, D. A. Prober, B. A. Edgar, R. N. Eisenman, P. Gallant, *Cell* **98**, 779 (1999).
15. D. A. Prober, B. A. Edgar, *Cell* **100**, 435 (2000).
16. M. A. Junger et al., *J. Biol.* **2**, 20 (2003).
17. O. Puig, M. T. Marr, M. L. Ruhf, R. Tjian, *Genes Dev.* **17**, 2006 (2003).
18. L. Cherbas, X. Hu, I. Zhimulev, E. Belyaeva, P. Cherbas, *Development* **130**, 2711 (2003).
19. E. J. Rulifson, S. K. Kim, R. Nusse, *Science* **296**, 1118 (2002).
20. T. Ikeya, M. Galic, P. Belawat, K. Nairz, E. Hafen, *Curr. Biol.* **12**, 1293 (2002).
21. T. E. Rusten et al., *Dev. Cell* **7**, 179 (2004).
22. We thank G. Jarretou for technical assistance; N. Tapon, J.-P. Vincent, M. Tatar, and P. Follette for comments on the manuscript; C. Mirth and P. Caldwell for communicating unpublished results; G. Adam for discussions; and L.-E. Zaragosi and J. Hopkins for assistance with quantitative real-time fluorescence polymerase chain reaction (QPCR). Supported by CNRS, INSERM, Association pour la Recherche contre le Cancer (grants 7696 and 3339), and Fondation de France.

Supporting Online Material

www.sciencemag.org/cgi/content/full/1119432/DC1
Materials and Methods
Figs. S1 and S2
References

29 August 2005; accepted 15 September 2005
Published online 22 September 2005;
10.1126/science.1119432
Include this information when citing this paper.

Small-Molecule Inhibitor of *Vibrio cholerae* Virulence and Intestinal Colonization

Deborah T. Hung,* Elizabeth A. Shakhnovich, Emily Pierson, John J. Mekalanos

Increasing antibiotic resistance requires the development of new approaches to combating infection. Virulence gene expression in vivo represents a target for antibiotic discovery that has not yet been explored. A high-throughput, phenotypic screen was used to identify a small molecule 4-[N-(1,8-naphthalimide)]-n-butyric acid, virstatin, that inhibits virulence regulation in *Vibrio cholerae*. By inhibiting the transcriptional regulator ToxT, virstatin prevents expression of two critical *V. cholerae* virulence factors, cholera toxin and the toxin coregulated pilus. Orogastic administration of virstatin protects infant mice from intestinal colonization by *V. cholerae*.

We are entering a challenging era where microbial resistance to antibiotics will complicate the treatment of nearly all common bacterial infections. The development of antimicrobials has lagged behind the development of antibi-

otic resistance for many life-threatening bacterial species. Current antimicrobials, for the most part, target a relatively small number of essential gene functions, such as inhibition of cell wall synthesis, DNA replication, RNA

transcription, protein synthesis, and folate synthesis. What development there has been has been largely limited to improving existing antibiotics through chemical modification and developing synergistic drugs that augment the efficacy of existing antibiotics. Nevertheless, a recent report identifying a new antituberculosis drug suggests it is still possible to identify entirely new classes of antibiotics (1).

Targeting the regulation of virulence factors of specific pathogens represents one approach to identifying antibiotics. Here we report the identification of a small molecule inhibitor of *Vibrio cholerae* virulence regulation and demonstrate its ability to inhibit bacterial colonization in an animal model of cholera.

Cholera is caused by the Gram-negative bacterium *V. cholerae*, which elaborates two major virulence factors, cholera toxin (CT) and the toxin coregulated pilus (TCP) (2). CT is an adenosine diphosphate-ribosylating toxin encoded in the genome of the filamentous, lysogenic CTX Φ phage. Secretion of CT into the intestinal lumen results in elevated cyclic adenosine monophosphate levels in intestinal epithelial cells and the subsequent secretory diarrhea that is the hallmark of the disease. TCP is thought to play a role in early attachment to intestinal epithelium and is required for intestinal colonization in an infant mouse model of cholera (2). The regulation of CT and TCP expression has been studied extensively (2), but the mechanisms by which environmental signals stimulate virulence expression *in vivo* are not clear.

We performed a high-throughput screen of a 50,000-compound small molecule library from Chembridge Research Laboratories (Microformats) to identify inhibitors of *V. cholerae* virulence factor expression. We constructed a screening strain of the classical biotype strain O395 that carries a chromosomally integrated tetracycline resistance gene (*tetA*) controlled by the cholera toxin (*ctx*) promoter. In a 384-well format, the strain was treated with 10 μ g/mL samples from the library to identify compounds that conferred tetracycline sensitivity when the strain was grown under *in vitro* conditions that would normally induce CT expression. We identified 109 compounds as inhibitors of *ctx* promoter activation by their ability to prevent *tetA* expression in the reporter strain. Fifteen of these compounds were notable for their inhibitory effects with minimal bacterial toxicity.

One of these 15 compounds, 4-[N-(1,8-naphthalimide)]-n-butyric acid (virstatin) (Fig. 1A) was selected for further study and was subsequently synthesized in gram quantities (3). We generated growth curves for two different *V. cholerae* biotype strains, O395 and

C6706, and showed that virstatin did not inhibit growth (50 μ M) (Fig. 1B). Minimal bactericidal concentrations (MBC) of 600 and 1200 μ M were determined for the two strains, respectively. We confirmed that under *in vitro* virulence-inducing conditions for these strains, CT production was undetectable in the presence of virstatin (50 μ M), as assayed by CT-enzyme-linked immunosorbent assay (CT-ELISA) (Fig. 1C). The minimal inhibitory concentrations for CT expression were 3 μ M and 40 μ M for O395 and C6706, respectively.

Because TCP is coregulated with CT, we examined virstatin's ability to inhibit the expression and function of TCP. Western blot analysis showed that the major subunit of TCP (TcpA) was not expressed under virulence-inducing conditions when either O395 or C6706 was treated with virstatin (Fig. 1C). Virstatin prevented the assembly of a functional pilus (TCP) in O395, as determined by its ability to prevent transduction of a bacteriophage (CTX-Km Φ) that uses TCP as its receptor (Fig. 1D) (4). CTX-Km Φ encodes kanamycin resistance and thus confers resistance when transduced into *V. cholerae*. Although 2.6×10^6 kanamycin-resistant colonies were obtained from phage transduction of O395 grown under virulence-inducing conditions, no kanamycin-resistant colonies were obtained when O395 was grown in the presence of virstatin, suggesting the absence of TCP on these cells.

We next examined whether virstatin affects known regulators of CT and TCP expression. In the canonical model for *V. cholerae* virulence regulation, environmental signals stimulate virulence by activating a cascading series of transcriptional regulators that ultimately induce transcription of the *ctx* and *tcp* genes (Fig. 2A) (5). The major role of regulators ToxRS and TcpPH is to activate transcription of *toxT*, which encodes an AraC-like transcriptional activator (6). ToxT activates multiple virulence genes (including *ctxAB*, *acfA*, and the *tcp* genes) and is autoregulated, presumably by self-inducing read-through transcription from the upstream *tcpA* promoter (7).

We investigated the effect of virstatin on these known virulence regulators by examining the transcription of *toxRS*, *tcpPH*, and *toxT* using transcriptional fusion reporters (Fig. 2B). In the presence of virstatin, the transcript levels of *toxRS*, *tcpPH*, and the most downstream gene, *toxT*, were all relatively unaffected, as determined by measuring β -galactosidase or β -glucuronidase activity. As expected, *ctx* transcription was notably decreased. Thus, virstatin blocks *ctx* transcription downstream of *toxT* transcription.

We also examined the effect of 50 μ M virstatin on *V. cholerae* global transcription patterns by using a genomic microarray (8). Eleven of 15 genes in O395 and 21 out of 22 genes in C6706 significantly repressed by virstatin (to

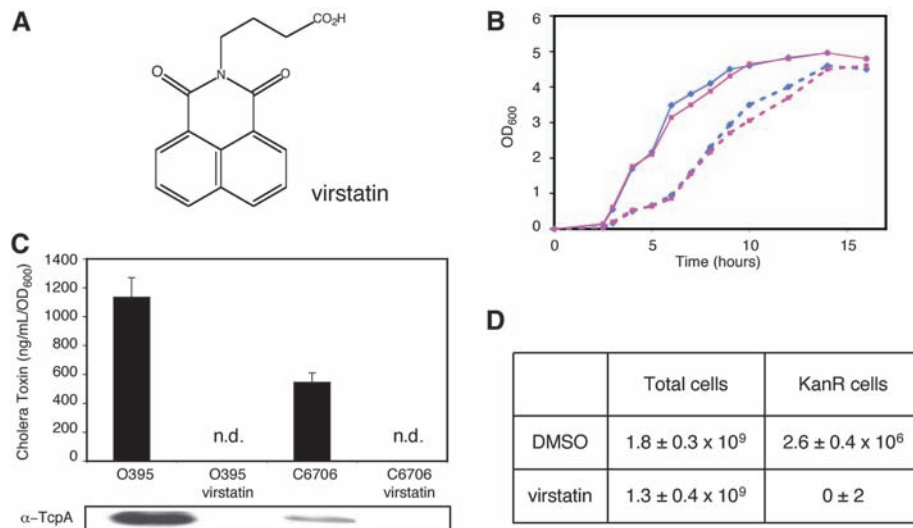


Fig. 1. Virstatin inhibits virulence expression in *V. cholerae*. (A) Chemical structure of virstatin. (B) Growth curves in LB at 37°C for O395 (dotted line) and C6706 (solid line). Dimethyl sulfoxide (DMSO) control, blue; virstatin, pink; OD₆₀₀, optical density measured at 600 nm. (C) CT and TcpA expression in the presence or absence of virstatin. Top: CT expression was measured by ELISA from O395 and C6706 in the presence of DMSO control or virstatin (50 μ M) after overnight growth under standard virulence-inducing conditions. Error bars represent the standard deviations from samples performed in triplicate. n.d., not detected. Bottom: TcpA expression was detected by Western blot with an α -TcpA antibody. (D) CTX-Km Φ transduction of O395 in the absence and presence of virstatin. Functional TCP was assayed by growing O395 to mid-log phase under virulence-inducing conditions (LB at pH 6.5 and 30°C) in the presence of DMSO control or virstatin (50 μ M). After 30 min incubation with phage, cultures were plated on LB-Kanamycin plates to enumerate transduction events. Total cells and kanamycin-resistant (KanR) cells were counted to reflect transduction efficiency. In the presence of virstatin, no transduction events were measured, which is a 6-log reduction compared to DMSO control.

Department of Microbiology and Molecular Genetics, Harvard Medical School, 200 Longwood Avenue, Boston, MA 02115, USA.

*To whom correspondence should be addressed. E-mail: dhung@partners.org

levels less than one-third of control levels) are within the *tcp* or *ctx* loci (3). These findings are consistent with the results obtained with transcriptional reporters, with ToxT regulating most genes that are down-regulated by virstatin. Moreover, in accordance with the established model for CT and TCP regulation, virstatin appears to inhibit ToxT post-transcriptionally.

Virstatin inhibited ToxT activity when ToxT was expressed under the control of a heterologous pBAD promoter, induced by arabinose, in *V. cholerae* strain O395 Δ *toxT* (Fig. 3A). To confirm that virstatin has no effect on ToxT expression, we constructed a *toxT* variant containing a C-terminal Myc₅ tag that both is active (albeit slightly less active than wild-type) and can be inhibited by virstatin (Fig. 3A) (3). Western blot analysis showed comparable levels of ToxT-Myc₅ expression in

the presence and absence of virstatin, confirming that the inhibition is post-translational.

Virstatin also inhibited ToxT induction of *ctx-lacZ* in *Escherichia coli* reporter strain DTH3060 free of all other *V. cholerae* factors that might otherwise affect *ctx* induction (Fig. 3B) (9, 10). When ToxT was expressed constitutively from plasmid pEP99.1 (3), β -galactosidase activity was induced 6 to 10 times more than in strain DTH3060 without and with control plasmid pJB658 (11). With virstatin present, this induction was suppressed to baseline levels. We obtained similar results using ToxT-Myc₅ (pEP99.2) and performed Western blot analysis to confirm that ToxT expression was not altered by virstatin.

A virstatin-resistant mutant of ToxT was isolated from a library of ToxT mutants by propagating pBAD*toxT* in the *E. coli* mutator

strain XL1-Red (Stratagene), transforming the resulting plasmid library into the reporter strain DTH3060, and screening the resulting colonies on LB agar containing virstatin, arabinose, Xgal, ampicillin, tetracycline, and kanamycin. One intensely blue colony was isolated from ~20,000 colonies screened, indicating a clone that expressed a ToxT mutant capable of inducing *ctx-lacZ* in the presence of virstatin. Sequencing of the *toxT* gene revealed a single point mutation, L113P, that occurs in the N-terminal, putative dimerization domain based on its sequence homology to other AraC-like proteins.

ToxT_{L113P} was resistant to virstatin when expressed in O395 Δ *toxT* with equivalent amounts of CT produced in the absence or presence of virstatin (50 μ M) (Fig. 3A). A similar phenomenon was observed in the heterologous *E. coli* strain DTH3060, with no inhibition of ToxT_{L113P} by increasing concentrations of virstatin (until 60 μ M), in stark contrast to the inhibition observed of wild-type ToxT (Fig. 3C). These data demonstrate that ToxT carrying a mutation in the N-terminal domain displays relative resistance to virstatin. Because the N-terminal domain of ToxT is its putative dimerization domain, virstatin may alter the dimerization state of ToxT, thus inactivating it.

In order to determine if the inhibition of virulence observed in vitro could affect in vivo infection, we tested the ability of virstatin to inhibit *V. cholerae* infection in an animal model. It has previously been shown that deletion of *toxT* attenuates TCP-dependent colonization of the small intestine of infant mice by *V. cholerae* (12).

We examined the effect of virstatin on the colonization of infant mice by *V. cholerae* strains that colonize in a TCP-dependent versus -independent manner. *V. cholerae* El Tor biotype strain C6706 was used as the TCP-dependent strain, because of its similar growth

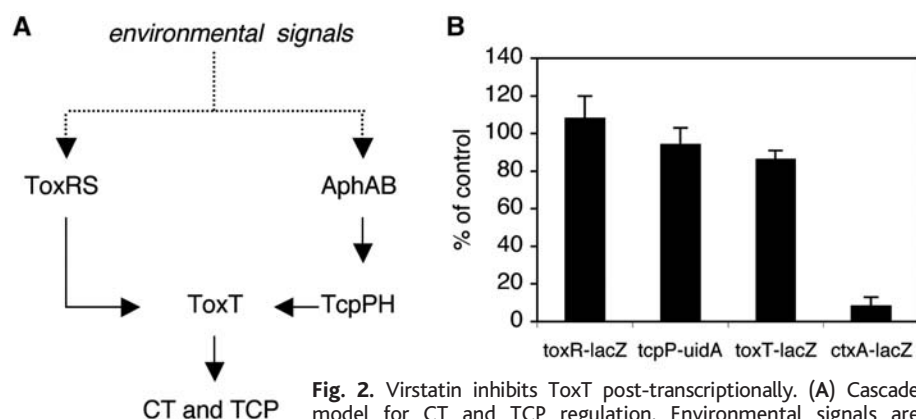


Fig. 2. Virstatin inhibits ToxT post-transcriptionally. (A) Cascade model for CT and TCP regulation. Environmental signals are transduced by AphAB, TcpPH, and ToxRS, of which the latter two transcriptionally activate *toxT*. ToxT then activates *ctx* and *tcp* transcription. (B) Virstatin inhibits *ctx* but not *toxR*, *tcpP*, or *toxT* transcription. Transcriptional reporter strains (O395) were grown overnight under virulence-inducing conditions (pH 6.5 and 30°C) in the presence of DMSO control or virstatin (50 μ M). Transcriptional fusions of *toxR*, *toxT*, and *ctxA* with *lacZ* were assayed for β -galactosidase activity. A transcriptional fusion of *tcpP* with *uidA* was assayed for β -glucuronidase activity. Data are presented as the percentage of reporter activity in the presence of virstatin compared to the DMSO control. Error bars represent the standard deviation for samples performed in triplicate.

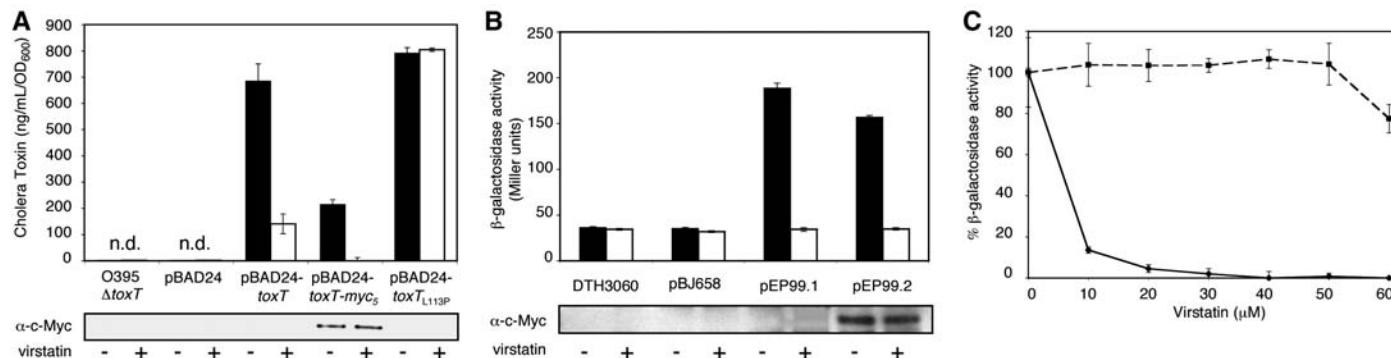


Fig. 3. Virstatin inhibits ToxT. (A) Top: Virstatin inhibits CT expression in O395 when ToxT is expressed under pBAD promoter control. O395 Δ *toxT*, O395 Δ *toxT* with pBAD24, pBAD24-*toxT*, pBAD24-*toxT-myc₅*, or pBAD24-*toxT_{L113P}* were induced (with 0.001% arabinose) in the presence of DMSO or virstatin (50 μ M). Virstatin inhibited CT expression in cells expressing wild-type and Myc-tagged ToxT but not ToxT_{L113P}. DMSO, black; virstatin, white. Bottom: Western blot with α -Myc demonstrates that virstatin does not alter ToxT-Myc₅ expression. (B) Top: Virstatin inhibits *ctx* transcription in *E. coli* reporter strain DTH3060 carrying *ctx-lacZ*, as measured by β -galactosidase activity. Constitutive ToxT (pEP99.1) and ToxT-Myc₅ (pEP99.2) expression

under *tet* promoter control resulted in 6 to 10 times more than in induction over control strain DTH3060 without or with control plasmid (pJB658). Virstatin repressed induction to control levels. DMSO, black; virstatin, white. Bottom: Western blot with α -Myc demonstrates that virstatin does not alter ToxT-Myc₅ expression. (C) Virstatin, at increasing concentrations, inhibited β -galactosidase activity in DTH3060 when wild-type ToxT but not ToxT_{L113P} was expressed (under pBAD promoter control; induced with 0.1% arabinose). Activity is presented as percentage of reporter activity in the presence of varying concentrations of virstatin compared to no virstatin. ToxT, solid line; ToxT_{L113P}, dotted line.

kinetics in the presence and absence of virstatin to TCP-independent *V. cholerae* strain S533. S533 is a non-O1 non-O139 clinical isolate that lacks the *toxT*, *tcp*, and *ctxAB* genes but is nevertheless able to colonize infant mice (13).

To validate comparison of the two strains, we examined their competitive capacity in vitro, in the presence and absence of virstatin, by growing S533 and C6706 together. The competitive index (CI) (14) of S533 versus C6706 was close to 1 in the presence and absence of virstatin (3).

Inoculation with single strains into the infant mouse in the presence of virstatin demonstrated a marked reduction in colonization of C6706 but not S533. Infant mice (5 to 6 days old) were orogastrically inoculated as previously described with *V. cholerae* strain C6706 or S533 (15) in the presence or absence of virstatin and killed at 18 to 24 hours (3). Small intestine homogenate from each mouse was plated on LB-agar containing streptomycin for enumeration of live bacterial counts. Under optimized conditions, S533 colonization was not affected by the presence of virstatin. How-

ever, C6706 colonization dropped by four logarithms in the presence of virstatin (Fig. 4A).

Competition experiments comparing the relative ratios of C6706 and S533 recovered after co-inoculation into the infant mouse showed the same selective effect of virstatin on C6706 but not S533 as the single-inoculation studies. A mixture of S533 and C6706 in the presence or absence of virstatin was orogastrically inoculated into infant mice. In the absence of virstatin, each mouse was colonized by both strains (CI 0.3 to 35). In contrast, in the presence of virstatin, very few C6706 colonies could be recovered. The CI of S533/C6706 increased over four logarithms (Fig. 4B). Thus, virstatin is able to significantly attenuate the TCP-dependent infection of C6706 relative to S533, a strain whose colonization is independent of ToxT and insensitive to the activity of virstatin.

Because virstatin's inhibition of ToxT and subsequent TCP expression is the likely cause of attenuation in C6706 colonization, we examined the ability of a C6706 Δ *tcpA* strain to compete with the wild type in the presence of virstatin (Fig. 4C). Mice were orogastrically inoculated

with or without virstatin and boosted again at 3 and 6.5 hours post-inoculation. Mice were killed at 2, 4.5, 7.5, and 24 hours post-inoculation. In the absence of virstatin, we observed the previously described, severely attenuated phenotype of the Δ *tcpA* strain (16) and were unable to recover any C6706 Δ *tcpA* bacteria at 24 hours, whereas C6706 wild-type colonized efficiently (Fig. 4C). However, in the presence of virstatin, recovery of wild-type C6706 was significantly diminished, and nearly equivalent numbers of Δ *tcpA* and wild-type bacteria were recovered at all time points (Fig. 4D). Thus, virstatin is able to eliminate wild-type C6706's competitive advantage over C6706 Δ *tcpA* during in vivo infection.

In vivo studies with C6706*toxT*_{L113P}, a mutant of wild-type C6706 carrying the mutation in the chromosome at the native *toxT* locus, confirmed that the differences in colonization are due to the effect of virstatin on ToxT. When inoculated alone, C6706*toxT*_{L113P} colonization was unaffected by the presence of virstatin (Fig. 4A). When inoculated together in the presence of virstatin, C6706*toxT*_{L113P} was able to colonize better than wild-type C6706 with a CI of 50 (Fig. 4B) [in vitro CI \sim 1, (3)]. Together, these data demonstrate that virstatin inhibits intestinal colonization specifically by blocking the activity of ToxT in vivo.

Finally, we examined whether virstatin could affect long-term infection if administered after colonization has already been established in the infant mouse model. This effect would be analogous to treatment of cholera patients with antibacterials such as tetracycline after the onset of diarrhea, which can reduce the duration of symptoms (17). We found that delayed administration of virstatin 12 hours after inoculation with C6706 still reduced the recovery of C6706 by over three logarithms relative to C6706 recovered from untreated infant mice (Fig. 4D). These data complement prior observations on the requirement of early in vivo virulence expression (18) and suggest that ongoing, late expression of ToxT-dependent genes is also necessary for optimal colonization in this animal model. This result also demonstrates that drugs such as virstatin, like conventional antibacterials, could have utility even after disease has been diagnosed.

Other small molecule inhibitors of virulence regulation have been reported, including inhibitors of a two-component regulator of alginate synthesis in *Pseudomonas aeruginosa* (19) and inhibitors of quorum sensing in *Staphylococcus aureus* (20) and *P. aeruginosa* (21). Inhibitors of virulence factors have also been explored, including compounds that block type III secretion in *Yersinia* (22) or anthrax toxin protease activity (23). Here we show that even in the absence of any chemical or target structural information, a high-throughput phenotypic screen can be used to identify small molecule virulence inhibitors that exhibit in vivo efficacy against bacterial infection after

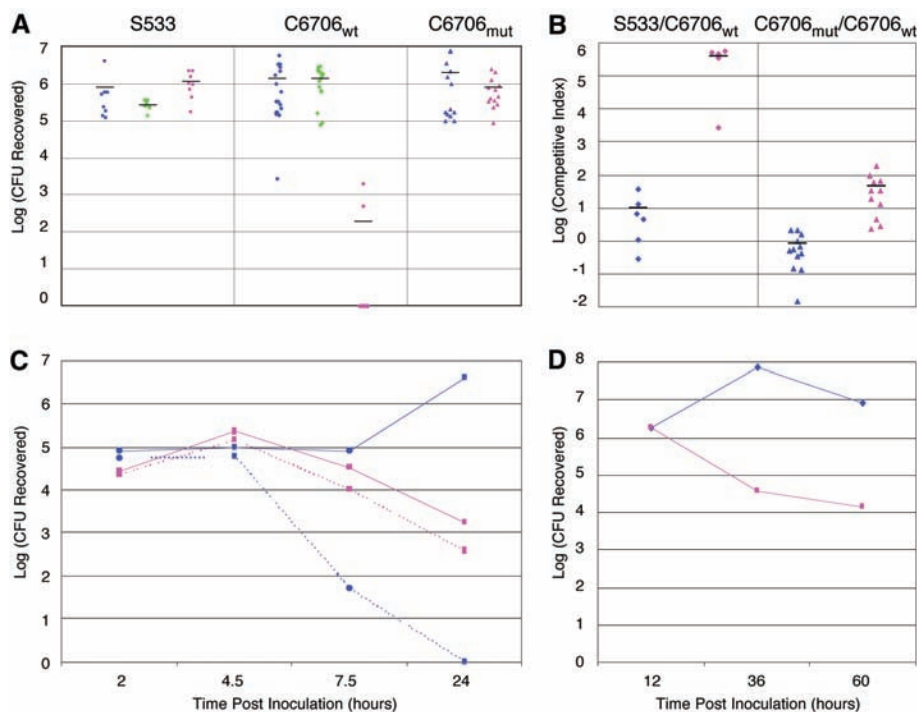


Fig. 4. Virstatin inhibits ToxT-dependent colonization of infant mice. (A) When inoculated alone, C6706 wildtype (C6706_{wt}) colonization was reduced 4 logs in the presence of virstatin under conditions that do not affect S533 or C6706*toxT*_{L113P} (C6706_{mut}) colonization. Bacteria were recovered from mice 18 to 24 hours post-oro-gastric inoculation and plated for enumeration. Each data point represents the output from a single animal and the bar represents the log of the geometric mean of data obtained from individual mice. Control buffer inoculum, no boost, blue; control buffer inoculum, control buffer boost, green; virstatin in both inoculum and boost, pink. CFU, colony-forming units. (B) When strains were co-inoculated, virstatin increased the CI of S533 versus C6706_{wt} by 4.5 logs, and the CI of C6706_{mut} versus C6706_{wt} by 1.5 logs. No virstatin, blue; virstatin, pink. (C) When C6706_{wt} and C6706 Δ *tcpA* were co-inoculated, virstatin decreased recovery of C6706_{wt} by 3 logs, down to the levels of C6706 Δ *tcpA*. Recovery of the two strains in the presence of virstatin at 24 hours was nearly 1:1, whereas no C6706 Δ *tcpA* was recovered from a competition experiment in the absence of virstatin. C6706_{wt}, solid; C6706 Δ *tcpA*, dotted; buffer, blue; virstatin, pink. (D) When C6706_{wt} infection was allowed to establish for 12 hours and mice then were treated with virstatin, colonization was reduced 3 logs in comparison to control buffer-treated mice. Control boost, blue; virstatin, pink.

simple orogastric administration. Thus, identification of inhibitors of virulence represents a path to anti-infective discovery that is quite different from conventional approaches that target only bacterial processes that are essential both in vivo and in vitro. We further predict that drugs such as virstatin may act synergistically with conventional antibiotics, because they act through independent mechanisms to block in vivo bacterial replication or survival.

References and Notes

1. K. Andries *et al.*, *Science* **307**, 223 (2005).
2. M. K. Waldor, J. J. Mekalanos, in *Enteric Infections and Immunity*, L. J. Paradise, Ed. (Plenum, New York, 1996), pp. 37–55.
3. Materials and methods are available as supporting material on Science Online.
4. M. K. Waldor, J. J. Mekalanos, *Science* **272**, 1910 (1996).
5. V. J. DiRita, *Mol. Microbiol.* **6**, 451 (1992).
6. D. E. Higgins, E. Nazareno, V. J. DiRita, *J. Bacteriol.* **174**, 6974 (1992).
7. R. C. Brown, R. K. Taylor, *Mol. Microbiol.* **16**, 425 (1995).
8. J. Bina *et al.*, *Proc. Natl. Acad. Sci. U.S.A.* **100**, 2801 (2003).
9. E. S. Krukonis, R. R. Yu, V. J. DiRita, *Mol. Microbiol.* **38**, 67 (2000).

10. DTH3060 is derived from *E. coli* strain VJ787 (*put::ctx-lacZ*) by deletion of *tolC*, an outer membrane porin, to confer greater sensitivity to virstatin.
11. J. M. Blatny, T. Brautaset, H. C. Winther-Larsen, P. Karunakaran, S. Valla, *Plasmid* **38**, 35 (1997).
12. G. A. Champion, M. N. Neely, M. A. Brennan, V. J. DiRita, *Mol. Microbiol.* **23**, 323 (1997).
13. Strain S533 was obtained from the Mekalanos lab collection of *V. cholerae* strain, originally isolated in 1981 from Soongnern Hospital in Thailand.
14. CI represents the ratio of test strain to wild type recovered from the intestine (or after overnight in vitro growth) divided by the ratio of input test strain to wild type. C6706 was marked with a *lacZ* mutation that does not affect colonization but allows it to be distinguished from S533 colonies by blue/white detection on LB-agar plates with Xgal. When the number of bacteria recovered were below the detection limit, 1 was chosen as the denominator to calculate the CI.
15. M. J. Angelichio, J. Spector, M. K. Waldor, A. Camilli, *Infect. Immun.* **67**, 3733 (1999).
16. R. K. Taylor, V. L. Miller, D. B. Furlong, J. J. Mekalanos, *Proc. Natl. Acad. Sci. U.S.A.* **84**, 2833 (1987).
17. G. H. Rabbani, M. R. Islam, T. Butler, M. Shahrier, K. Alam, *Antimicrob. Agents Chemother.* **33**, 1447 (1989).
18. S. H. Lee, D. L. Hava, M. K. Waldor, A. Camilli, *Cell* **99**, 625 (1999).
19. S. Roychoudhury *et al.*, *Proc. Natl. Acad. Sci. U.S.A.* **90**, 965 (1993).

20. J. S. Wright III, R. Jin, R. P. Novick, *Proc. Natl. Acad. Sci. U.S.A.* **102**, 1691 (2005).
21. M. Hentzer *et al.*, *EMBO J.* **22**, 3803 (2003).
22. A. M. Kauppi, R. Nordfelth, H. Uvell, H. Wolf-Watz, M. Elofsson, *Chem. Biol.* **10**, 241 (2003).
23. B. E. Turk *et al.*, *Nat. Struct. Mol. Biol.* **11**, 60 (2004).
24. We thank the National Cancer Institute's Initiative for Chemical Genetics (S. L. Schreiber, P.I.) and the Harvard Institute of Chemistry and Cell Biology for their support of and assistance with the high-throughput small molecule screen; the New England Regional Center of Excellence in Biodefense and Infectious Disease Research for its continued support of research activities involving the identification of small molecule inhibitors of bacterial virulence; and S. Chiang, J. Mougous, and J. Zhu for review of the manuscript. Supported by NIH grant nos. K08 AI060708-01 (D.T.H.) and AI26289 (J.J.M.) and by an NSF predoctoral fellowship (E.A.S.).

Supporting Online Material

www.sciencemag.org/cgi/content/full/1116739/DC1
 Materials and Methods
 SOM Text
 Tables S1 to S3
 References and Notes

29 June 2005; accepted 22 September 2005
 Published online 13 October 2005;
 10.1126/science.1116739
 Include this information when citing this paper.

The V-Antigen of *Yersinia* Forms a Distinct Structure at the Tip of Injectisome Needles

Catherine A. Mueller,^{1*} Petr Broz,^{1*} Shirley A. Müller,^{1,2}
 Philippe Ringler,^{1,2} Françoise Erne-Brand,^{1,2} Isabel Sorg,¹
 Marina Kuhn,¹ Andreas Engel,^{1,2} Guy R. Cornelis^{1,†}

Many pathogenic bacteria use injectisomes to deliver effector proteins into host cells through type III secretion. Injectisomes consist of a basal body embedded in the bacterial membranes and a needle. In *Yersinia*, translocation of effectors requires the YopB and YopD proteins, which form a pore in the target cell membrane, and the LcrV protein, which assists the assembly of the pore. Here we report that LcrV forms a distinct structure at the tip of the needle, the tip complex. This unique localization of LcrV may explain its crucial role in the translocation process and its efficacy as the main protective antigen against plague.

Type III secretion (T3S) is commonly used by Gram-negative pathogenic bacteria to introduce effector proteins into target host cells (1). *Yersinia pestis* and *Y. enterocolitica*, causing bubonic plague and gastroenteritis respectively, share the same T3S system consisting of the Ysc (Yop secretion) injectisome, or “needle complex,” and the secreted Yop (Yersinia outer protein) effector proteins. Three translocator proteins, YopB, YopD, and LcrV, are necessary to deliver the effectors across the target cell membrane (2–5). LcrV is required for the correct assembly of the

translocation pore formed by YopB and YopD in the membrane of the target cell (2, 6). LcrV (also known as V antigen) is a soluble protein important for virulence (7) and is a protective antigen against plague (8). Antibodies against LcrV prevent the formation of the translocation pore (6) and block the delivery of the effector Yops (9). The injectisome is composed of a basal body resembling that of the flagellum and a needle (10). The needle has a helical structure (11) and in *Yersinia* is formed by the 9.5-kD protein YscF (12, 13).

Transmission electron micrographs of the surface of *Y. enterocolitica* E40 bacteria suggested that the injectisome needle ends with a well-defined structure (fig. S1). To characterize this structure, we purified needles from multi-effector knockout bacteria (strain ΔHOPEMT) that had been incubated under either secretion-

permissive or -nonpermissive conditions (14), then analyzed them by scanning transmission electron microscopy (STEM). A distinct “tip complex” was observed for the wild-type needles, comprising a head, a neck, and a base (Fig. 1A, arrow, and fig. S2A). The tip structure was the same in both cases, but more needles were produced under secretion-permissive conditions (15). The purified needle fraction from secreting bacteria was analyzed to determine the components of the tip complex (fig. S3A). LcrV, YopD, and the needle subunit YscF were found. Other proteins included flagellins, which are usual contaminants of needle preparations (13). Upon cross-linking of purified needles, products formed between YscF and LcrV, suggesting that the latter is a structural component of the needle (fig. S3B).

The tip complex observed for wild-type needles was absent from needles prepared from bacteria deprived of LcrV (ΔHOPEMNQ) (table S1) (16). Instead, this end of the needle was distinctly pointed (Fig. 1B, asterisk, and fig. S2B). The tip complex was restored after the mutation was complemented in trans with *lcrV*⁺ (Fig. 1B, right, and fig. S2B). Needles from single *yopN* or *yopQ* knockout bacteria were analyzed as controls and displayed the same tip complex as the wild-type needles (fig. S4). Thus, the formation of the tip complex involved LcrV but not YopN or YopQ.

Needles from a *yopBD* double mutant (15) were analyzed to exclude the possibility that YopD and, although not detected on the gels, the third translocator protein YopB were tip complex components. The appearance of the tip complex was unchanged (fig. S4).

When wild-type needles were incubated with affinity-purified polyclonal antibodies to LcrV, the latter specifically bound to the tip

¹Biozentrum der Universität Basel and ²Maurice E. Müller Institute, Klingelbergstrasse 50-70, CH-4056, Basel, Switzerland.

*These authors contributed equally to this work.
 †To whom correspondence should be addressed.
 E-mail: guy.cornelis@unibas.ch